



The promoting role of bismuth for the enhanced photocatalytic oxidation of lignin on Pt-TiO₂ under solar light illumination

Jianyu Gong*, Alexander Imbault, Ramin Farnood*

Department of Chemical Engineering and Applied Chemistry, University of Toronto, Toronto, Ontario, M5S 3E5, Canada

ARTICLE INFO

Article history:

Received 31 August 2016

Received in revised form 4 November 2016

Accepted 21 November 2016

Available online 22 November 2016

Keywords:

Bismuth

Platinum

TiO₂

Selective oxidation

Lignosulfonate

ABSTRACT

In this work, bismuth (Bi) and platinum (Pt) were utilized to promote the oxidation of lignosulfonate over TiO₂ under solar light illumination at facile condition. The characterization results revealed the presence of Bi and Pt covering on TiO₂ surface with zero valent state. And, the Bi1%Pt1%-TiO₂ photocatalyst performed excellent reactivity in oxidation of lignosulfonate to produce valuable compounds and CO₂ due to the generation of photo-generated hole (h⁺) and superoxide radicals (O₂^{•-}), which were confirmed by quenching experiments. After 1 h of photocatalytic reaction, almost 85% of lignosulfonate was converted into guaiacol, vanillic acid (VA), vanillin, 4-phenyl-1-buten-4-ol and other intermediates that were identified and quantified using HPLC. We found that the amount ratio of added Bi and Pt was the essential effect to the oxidative efficiency of lignin due to the produced additional active sites on TiO₂ surface. This study provides a new strategy for generating h⁺ and O₂^{•-} radicals under solar light and suggests its application for the selective oxidation of lignin.

© 2016 Elsevier B.V. All rights reserved.

1. Introduction

With the increasing concerns over the long term effects of global climate change and depletion of fossil fuels, there has been a growing interest to use lignocellulosic biomass for the production of chemicals and fuels [1,2]. However, sustainable operation of lignocellulosic bio-refineries is pending on the development of cost effective and robust integrated processes that fully utilize cellulose, hemicellulose and lignin.

As a natural aromatic biopolymer, lignin provides a unique opportunity for the production of aromatic chemicals and fuels. Accordingly, there has been a surge of interest in exploring new ways to convert lignin; that constitutes about 15%–35% of lignocellulosic biomass, to value-added products [3]. Among those valuable products, vanillin and vanillic acid are widely utilized as a flavoring or functional ingredient in food and cosmetic products [4,5]. Guaiacol is also used as an important raw material in production of medical compounds, dyestuff synthesis and bio-oil industry [6–8].

Gasification, pyrolysis, oxidation, hydro-processing, acid or base catalyzed de-polymerization, and liquid phase reforming, are

some of various processes that has been reported in the literature for lignin conversion [9].

Considering the existing processes for lignin valorization, selective catalytic processes for the transformation of lignin at low-temperature and facile condition is expected to offer a significant economic advantage. Low temperature photocatalytic oxidation of lignin under ultraviolet (UV) illumination and the role of reactive species, such as •OH, O₂^{•-}, ¹O₂ and photogenerated hole (h⁺) radicals in this process have been investigated previously [10]. Photocatalytic transformation of lignin using hetero-nanostructured solar photocatalysts by combining semiconductors with noble metals, secondary semi-conductors, or by doping with metal or nonmetal atoms have been also examined [11–13]. Among those photocatalysts, noble metals-based materials, such as Pt/TiO₂ [14,15], Ag-AgCl/ZnO [16] and Pd/TiO₂ [17,18], have received growing attention for the selective oxidation of organic compounds.

Recently, a promising class of bismuth (Bi) promoted Pt- or Pd-based photocatalysts has been reported for the selective oxidation of chain alcohols or aromatic compounds [19–21]. The roles of bismuth in these catalysts have been suggested to be through one of several mechanisms including: (1) blocking of active sites through steric hindrance [22]; (2) generation of bismuth based alloy [23]; (3) protecting the noble metals from over oxidation [22]; (4) forming a new active center like Bi-OH_{ads} [24]; and (5) existing of soluble Bi species in reaction system [25,26].

* Corresponding authors.

E-mail addresses: jygong@hust.edu.cn (J. Gong), [\(R. Farnood\).](mailto:ramin.farnood@utoronto.ca)

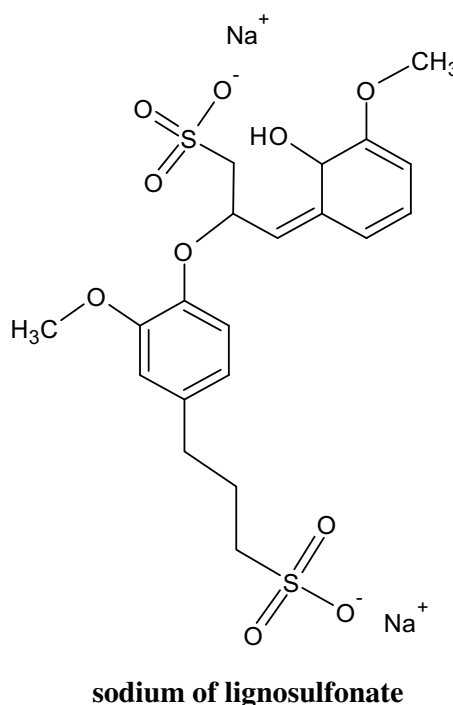


Fig 1. The molecular structure of sodium of lignosulfonate.

In this work, Bi and Pt co-modified TiO₂ was used for selective oxidation of lignin resulting in the generation of valuable compounds. The photocatalytic performance and structural properties of Bi/Pt-TiO₂ were estimated to understand the role of Bi and Pt in the photocatalytic process. A parallel study has also been carried out to confirm the dominant generated reactive oxygen species (ROS) from photocatalysts in photocatalytic process by degradation of methyl orange (MO) in the presence of several scavengers. These photocatalysts were characterized by X-ray diffraction (XRD) and X-ray photoelectron spectroscopy (XPS) before and after the oxidation of lignin.

2. Experimental

2.1. Materials and chemicals

Lignin (sodium of lignosulfonate, as shown in Fig. 1), titanium dioxide (P25), bismuth nitrate (Bi(NO₃)₃·5H₂O), chloroplatinic acid hexahydrate (H₂PtCl₆·6H₂O), sodium borohydride (NaBH₄), sodium fluoride (NaF), 1,4-benzoquinone (BQ), triethanolamine (TEA), isopropanol (IPA), absolute ethanol, HCl and NaOH were purchased from by Sigma-Aldrich. All chemical reagents were of analytical grade and used without further purification. Ultrapure water (resistivity >18 MΩ·cm) obtained from a water purification system (Millipore, France) was used.

2.2. Characterizations

A Quanta 200 SEM was employed to characterize the morphology of the nanoparticles. The phase detection and analysis were performed by XRD (Rigaku Miniflex 600) using Cu K α radiation. The XPS analysis was conducted on a Thermo Scientific K-Alpha.

2.3. Photocatalyst preparation

The synthesis of Pt/Bi-TiO₂ was performed by using a reduction method. In brief, 1 g of P25 and the designed amount of BiNO₃·5H₂O

(1%, atomic ratio of Bi to Ti) and H₂PtCl₆·6H₂O (1%, atomic ratio of Pt to Ti) were added together in 10 mL of water. The mixture was stirring for 15 min and then 5 mL of NaBH₄ solution (1 M) was added dropwise into the mixture. After a continuous stir for another 15 min, the obtained gray powder was washed with ethanol and water, and then dried at 80 °C under H₂ atmosphere for 2 h. The final obtained particle was Pt/Bi-TiO₂. To produce Pt-TiO₂ or Bi-TiO₂, we used the same method mentioned above without adding Bi(NO₃)₃·5H₂O or H₂PtCl₆·6H₂O, respectively. All samples were kept in a vacuum storage to avoid oxidation until we used them.

2.4. Experimental procedure

The photocatalytic oxidation of lignin was conducted at room temperature. Catalyst (1 g/L) was added to 100 mL of a lignin (100 mg/L) solution in a 200-mL self-designed glass reactor with a quartz window. The suspension was equilibrated in the dark condition for 15 min prior to illumination. The photocatalytic activity of all as-prepared samples was evaluated under 300 W Xe lamp. The solar light intensity measured with a visible-light radiometer (Model: FZ-A, China), was 125 mW/cm². The photocatalytic reactions were monitored by sampling at designed time and filtered through a 0.22 μm PTFE filter to remove particles. Quenching experiments were performed similar to the degradation experiments except that radical scavengers, IPA (2 mM), NaF (2 mM), NaN₃ (2 mM), TEA (2 mM) and BQ (2 mM), were added to the reaction systems to investigate the contributory roles of reactive oxygen species (ROS) in the reactions. The pH values were adjusted by H₂SO₄ or NaOH. All batch experiments were done in duplicate. To analyze the stability of nanoparticles, the oxidation of lignin was repeated three times. After the first reaction, catalyst was washed with water twice and collected by centrifugation, then placed into fresh lignin solution for the next run.

The conversion of lignin, the yield of intermediates and the selectivity of those by-products were defined as follows:

$$\text{Conversion}(\%) = (\text{C}_0 - \text{C}_{\text{lignin}}) \times 100 / \text{C}_0$$

$$\text{Yield}(\%) = \text{C}_{\text{oxydate}} \times 100 / \text{C}_0$$

Where C₀ is the initial concentration of lignin; C_{lignin} is the concentration of lignin at sampling time; and C_{oxydate} is the concentration of the generated oxydate at given time, respectively.

2.5. Analytical methods

Samples were collected (0.5 mL for each sample) at given intervals using a 1 mL glass syringe and immediately filtered through

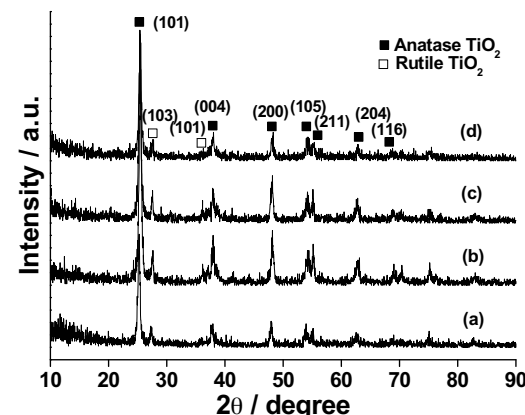


Fig. 2. XRD patterns of (a) TiO₂, (b) Bi1%-TiO₂, (c) Pt1%-TiO₂ and (d) Bi1%/Pt1%-TiO₂.

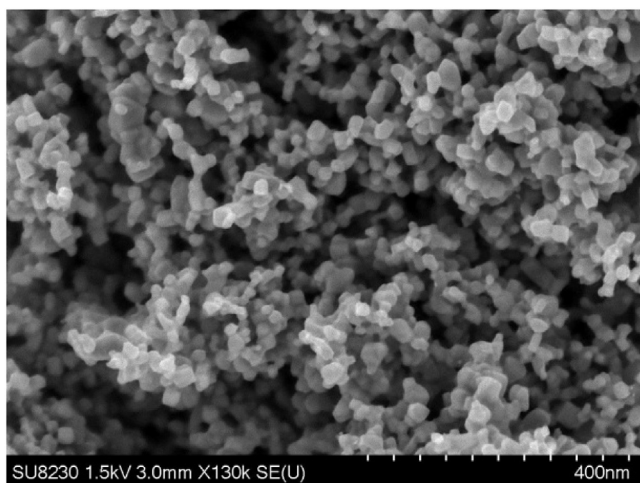


Fig. 3. SEM image of Bi1%Pt1%-TiO₂.

a 0.22 µm PTFE filter for high performance liquid chromatography (HPLC). The organic compounds were quantitatively analyzed using HPLC on a Perkin Elmer 785A equipped with a ODS HYPER-SIL C-18 column (250 mm × 4.6 mm × 5 µm). The determination was carried out under the following conditions: temperature 30 °C, mobile phase mixed water and acetonitrile (40:60 v/v), flow rate of 0.6 mL/min and injection volume of 20 µL. The UV absorption peak of lignin was observed at 280 nm that was assigned to aromatic ring groups [27,28].

2.6. Photoelectrochemical characterization

The photocurrent of photocatalysts was conducted with an electrochemistry station (IVIUM, Inc., USA) in a conventional three-electrode system containing 0.1 M Na₂SO₄ under solar light illumination. A saturated calomel electrode (SCE) and a platinum plate acted as reference electrode and counter electrode, respectively. The working electrode was prepared on a fluorine-doped tin oxide (FTO) conductive glass covered with 1 cm² of conductive carbon adhesive tape, and then the sample (20 mg) was dispersed on this area. The transient photocurrent response of the working electrode was measured at a +0.5 V bias potential. All potentials were referred to SCE.

3. Results and discussions

3.1. Characterization of catalysts

The crystal structures of neat TiO₂, and those containing 1% bismuth (Bi1%-TiO₂), 1% platinum (Pt1%-TiO₂), and 1% bismuth as well as 1% platinum (Bi1%Pt1%-TiO₂) were investigated using XRD, as shown in Fig. 2. For all samples, the XRD peaks at 27.4 and 36.1° were the characteristic peaks of rutile TiO₂ [29]. All other XRD peaks represent the characteristic peaks of the anatase phase of TiO₂ (JCPDS no.21-1272). There was no trace of any impurity on

Table 1

Photocatalytic oxidation of lignin under solar light illumination after 1 h of treatment over different photocatalysts.

Nanoparticles	Lignin Conversion (%)	Guaiacol Yield (%)	VA Yield (%)	Total Yield (%)
TiO ₂	54.5	8.7	0	8.7
Bi1%-TiO ₂	16.9	0	0	0
Pt1%-TiO ₂	28.2	0	0	0
Bi1%Pt1%-TiO ₂	84.5	22.7	0.5	23.2

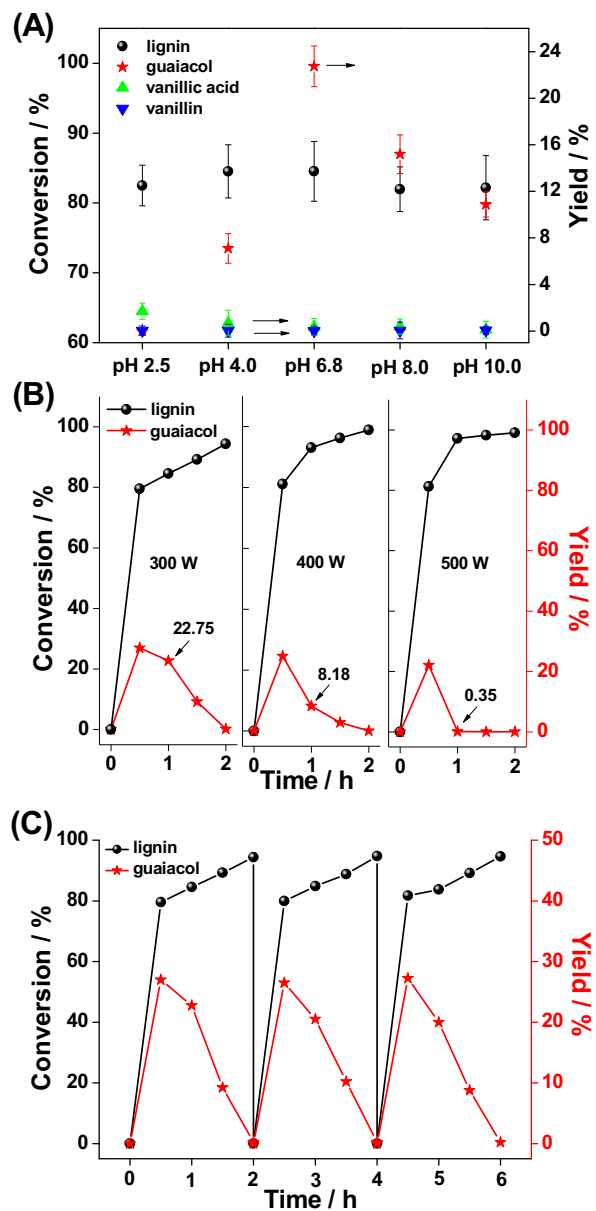


Fig. 4. The effects of (A) pH, (B) light intensity and (C) stability of photocatalyst on the photocatalytic oxidation of lignin over Bi1%Pt1%-TiO₂. For the case (A), the results were obtained for 1 h of reaction.

the Bi/Pt-TiO₂ sample, indicating that the added Bi and Pt did not affect the crystalline structure of TiO₂. Notably, no diffraction peaks for Bi or Pt were observed in the Bi/Pt-TiO₂ composite catalyst, which might be due to the low amount and uniform dispersion of Bi and Pt in these samples. Furthermore, the crystal phase of Bi/Pt-TiO₂ remained nearly unaffected even after three times use for the selective photocatalytic oxidation of lignin, as shown in Fig. S1. This conclusion was further confirmed by XPS analysis, as discussed in subsequent sections. The morphology of Bi/Pt-TiO₂ sample was observed using SEM in Fig. 3. It could be seen that particles were well dispersed and the average particle size was in the range of 100–200 nm. On the other hand, the added Bi or Pt in these nanoparticles could not be observed by EDX (data not shown) because of the low concentration of these dopants.

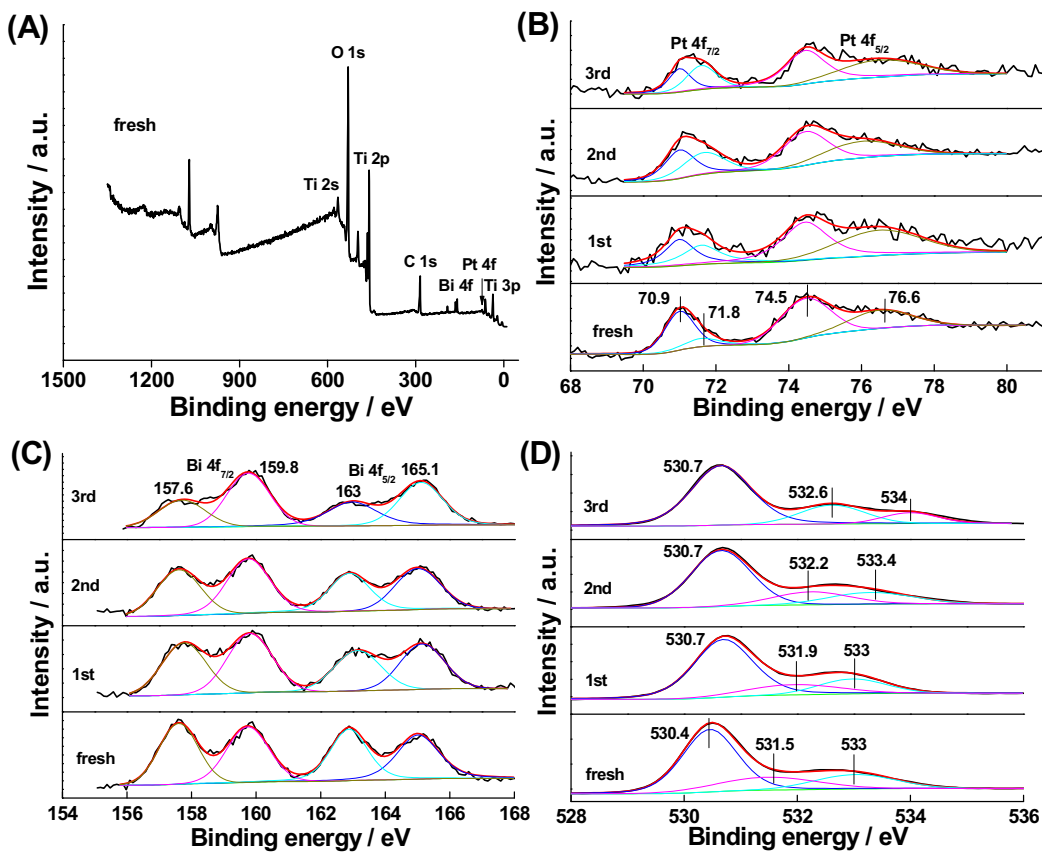


Fig. 5. High resolution XPS spectra of fresh Bi1%/Pt1%-TiO₂ and re-used Bi1%/Pt1%-TiO₂ samples: (A) full range; (B) Pt 4f; (C) Bi 4f and (D) O 1s.

3.2. Photocatalytic oxidation of lignin

3.2.1. Effect of photocatalyst on lignin oxidation

Lignin is consisting of methoxylated phenylpropane structures. P-coumaryl, coniferyl and sinapyl alcohols have been confirmed as main monomers in lignin, and they were linked by C–O and C–C bonds [30]. So, the selective cleavage of these linkages is crucial for the transformation of lignin to aromatics.

Photocatalytic oxidation of lignin was carried out under solar light irradiation over different photocatalysts, as shown in Table 1 Fig. S2 and Table S1. These results show that Bi1%/Pt1%-TiO₂ achieved the highest conversion of lignin (84.5%) and the highest total yield of byproducts (23.2%) after 1 h of treatment. Meanwhile, HPLC analysis showed that the main reaction products included guaiacol, vanillic acid and vanillin and 4-phenyl-1-buten-4-ol. Many other intermediates were also observed, but their concentrations were low (<0.1%) hence are not discuss in this paper. The pure TiO₂ would also oxidize 54.5% of lignin accompanying with 8.7% of yield of guaiacol, but no other major product was detected for this photocatalyst. In the Bi-TiO₂ and Pt-TiO₂ system, the conversion of lignin were only 16.89% and 28.23%, respectively, and the concentration of the related intermediates were too low to be reliably determined using the analytical method used in this study.

3.2.2. Effect of initial pH, light intensity and stability of photocatalyst on lignin oxidation

The effect of initial solution pH on photo-oxidation of lignin using Bi1%/Pt1%-TiO₂ under solar light irradiation for 60 min was determined. The lignin solution without pH adjustment (pH 6.8) was used as control. As shown in Fig. 4A, pH had little effect on the overall lignin conversion. The conversation of lignin at pH 2, 4,

6.8, 8, 10 were 82.5%, 84.5%, 84.5%, 81.9% and 82.2%, respectively. However, the selectivity of photocatalyst was significantly affected by the pH. The yield of guaiacol increased from 0% at pH 2 to a maximum of 22.7% at pH 6.8 before decreasing again to 10.9% at pH 10. In contrast, the highest production of vanillic acid (1.7%) was observed under acidic condition (pH 2.5). Earlier studies have suggested that the degradation of lignin degradation is enhanced under alkaline condition due to ease of breakage of the aromatic ring [31]; however, no consistent conclusions could be drawn for the selective oxidation of lignin.

Fig. 4B shows the oxidation of lignin under different light intensity. High light intensity improved the conversion rate of lignin but it also accelerated the decomposition of these intermediates implying that high light intensity was not suitable for the selective oxidation of lignin. As discussed in subsequent sections, this finding could be explained by the large amount of reactive radicals generated during the photocatalytic process.

3.2.3. Stability of photocatalyst

The stability of Bi1%/Pt1%-TiO₂ was also investigated by reusing of the photocatalyst. As shown in Fig. 4C, the conversion of lignin and the generation of guaiacol were practically unchanged after 3rd times reusing of Bi1%/Pt1%-TiO₂. To further understand the chemical valance change on the re-used Bi1%/Pt1%-TiO₂, XPS observing was conducted. The XPS of fresh Bi/Pt-TiO₂ provided in Fig. 5A revealed that the sample was mainly composed of Ti, Bi, Pt, O and a trace amount of C elements (C element come from the reference sample). In Fig. 5B, the binding energies of approximately 70.9 eV and 74.5 eV were attributed to Pt 4f_{7/2} and Pt 4f_{5/2} of bulk Pt metal (Pt⁰), while the other peaks at approximately 71.8 and 76.6 eV were assigned to the platinum oxide layer (Pt²⁺), which covered the

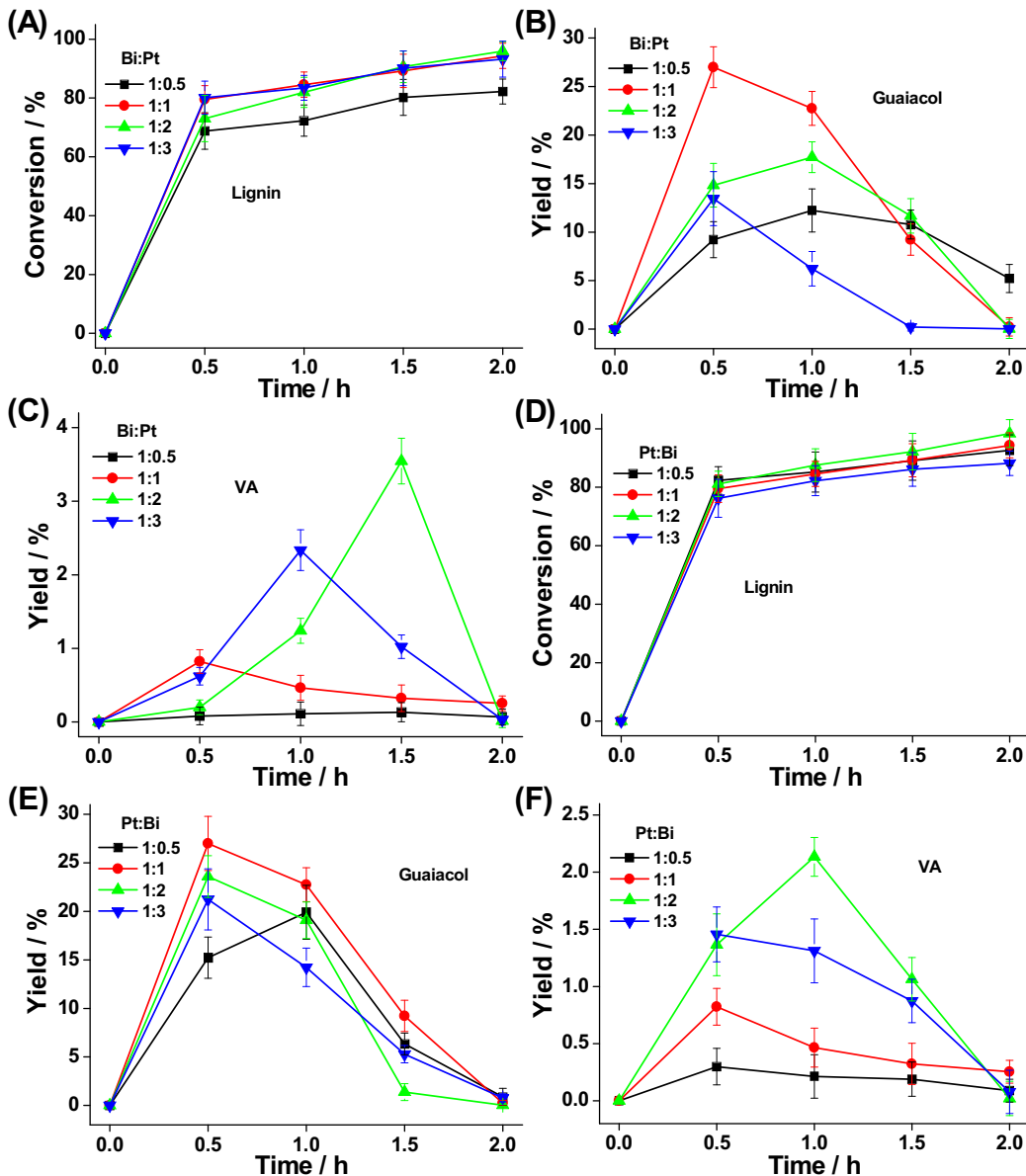


Fig. 6. (A) Conversion of lignin, (B) guaiacol and (C) VA yield in photocatalytic oxidation along with the reaction time catalyzed by Bi/Pt_x-TiO₂; and (D) conversion of lignin, (E) guaiacol and (F) VA yield in photocatalytic oxidation along with the reaction time catalyzed by Bi_x/Pt-TiO₂. (x = 0.5, 1, 2 and 3).

surface of bulk Pt metal particles [32,33]. For these reused samples, the main compound was still governed by bulk Pt metal, while the ratio of Pt²⁺ covered on bulk Pt metal surface increased slightly.

Fig. 5C showed high resolution Bi 4f XPS spectra of these samples. The peaks at 157.6 eV and 163 eV were attributed to Bi 4f_{7/2} and Bi 4f_{5/2} of Bi⁰, respectively, while the other two peaks at approximately 159.8 eV and 165.1 eV were assigned to Bi 4f_{7/2} and Bi 4f_{5/2} of Bi³⁺ [34]. For the three-time re-used Bi1%Pt1%-TiO₂ sample, Bi⁰ decreased slightly while Bi³⁺ increased. The O 1 s spectra of these samples (Fig. 5D) shows that the O 1 s peak could be deconvoluted into three separated peaks, two of which (i.e. peaks at 530.4 eV and 531.5 eV) might be attributed to lattice oxygen in the multi-phase photocatalysts, while the third one at 533 eV was ascribed to adsorbed oxygen [35]. For the reused samples, it was found that photocatalytic reaction had little influence on the chemical valence of photocatalysts. Therefore, based on the results of XRD and XPS, the existence of bulk Pt and bulk Bi in the Bi1%Pt1%-TiO₂ sample was confirmed.

3.2.4. Effect of amount ratio of Bi to Pt on TiO₂ for lignin oxidation

To examine the effect of Bi and Pt percentages on the activity of Bi/Pt-TiO₂, Bi1%Pt_x-TiO₂ and Bi_x/Pt1%-TiO₂ (x = 0.5, 1, 2 and 3) were considered. Fig. 6A shows that the conversion of lignin on Bi1%Pt_x-TiO₂ was not strongly depended on the Pt percentage. However, the generation of guaiacol and VA were affected by the amount of Bi and Pt. Fig. 6B shows that the highest yield of guaiacol (22.7%) was achieved on Bi1%Pt1%-TiO₂ within 1 h. Meanwhile, the generation of VA increased with Pt content till 2% but decreased as the Pt amount further increased to 3% (Fig. 6C). The maximum concentration of VA (3.5%) was obtained at 1.5 h of oxidation over Bi1%Pt2%-TiO₂. A clear decrease in the yield of VA (2.3%) was observed at high Bi content up to 3%, probably due to the surface blocking on Pt surface.

Similarly, Fig. 6D shows that there was no significant difference in the conversion of lignin over Bi_x/Pt1%-TiO₂ as x varied from 0.5 to 3%. According to Figs. 6E and 6F, the highest yield of guaiacol was achieved on Bi1%Pt1%-TiO₂ while the highest yield of VA (2.2%) was

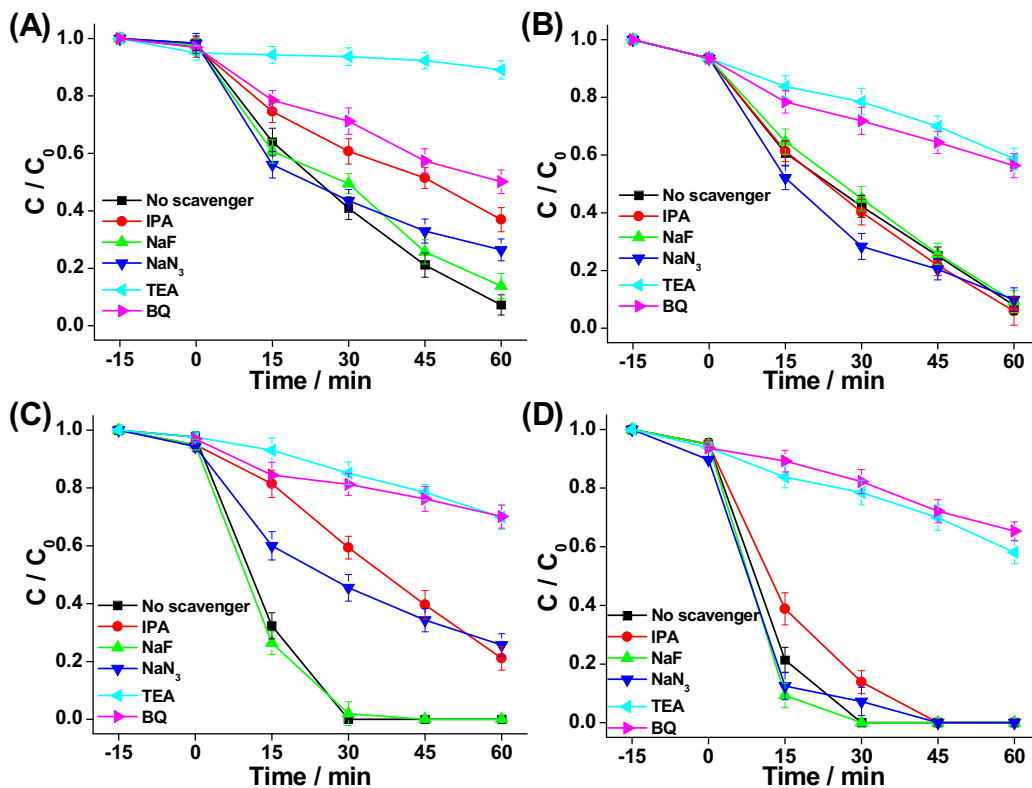


Fig. 7. Effects of varied scavenger conditions on the photocatalytic degradation of MO with (A) Pure TiO₂, (B) Bi1%-TiO₂, (C) Pt1%-TiO₂ and (D) Bi1%/Pt1%-TiO₂.

achieved on Bi2%/Pt1%-TiO₂ after 1 h of reaction, respectively. But higher Bi content was not beneficial for the VA production.

Higher guaiacol selectivity of Bi1%/Pt1%, may be explained considering that the photocatalytic oxidation of lignin on Bi/Pt-TiO₂ involves: 1) the decomposition of lignin and the intermediate compounds on Pt; and 2) the selective oxidation of lignin due to the presence of Bi. Increasing Pt likely increased the number of active sites resulting in improved hole-electron separation and hence the photocatalytic activity of Bi/Pt-TiO₂. This, however, also resulted in a greater degradation of byproducts and hence lower guaiacol formation. On the other hand, higher Bi content is expected to block Pt active sites and hence improve the selective degradation of lignin to guaiacol.

3.2.5. Mechanism analysis

In order to understand the mechanism of the photocatalytic oxidation of lignin, the main ROS generated during this process were investigated by quenching tests. In these experiments IPA, NaF, NaN₃, TEA and BQ were used as scavengers of •OH_{bulk}, •OH_{ads}, ¹O₂, h⁺ and O₂^{•-}, respectively [36–38]. To avoid possible interaction of scavengers with the photo-oxidation by-products of lignin, MO (10 mg/L) was selected as the target compound. For reference, photocatalytic degradation of MO using TiO₂, Bi1%-TiO₂, Pt1%-TiO₂ and Bi1%/Pt1%-TiO₂ are provided in Fig. S3. Control experiments confirmed that MO was not degraded in the absence of photocatalyst, suggesting that the degradation of MO by direct photolysis was negligible.

As shown in Fig. 7A, upon TEA addition, the degradation of MO in the presence of TiO₂ reduced from 93% to 11% after 1 h illumination, indicating the significance of h⁺ in the photo-oxidation process. And, the degradation rate of MO was also inhibited in the presence of BQ and IPA, implying that the role of O₂^{•-} and •OH_{bulk} in the TiO₂ photo-oxidation process. In our work, O₂^{•-} was readily generated from molecular oxygen in the reactor by capturing

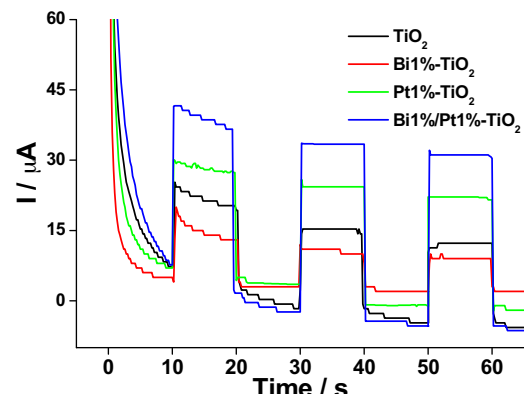


Fig. 8. Photocurrent responses of different photocatalysts at a bias potential of +0.5 V under solar light illumination.

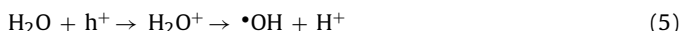
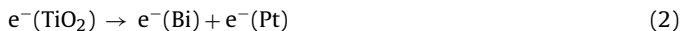
the photo-induced electrons. Finally, only a weak inhibition was observed with the addition of NaN₃ or NaF. This could be inferred that the role of ¹O₂ and •OH_{bulk} could be ignored in TiO₂ system. According to Figs. 7B to D, in the presence of Bi both h⁺ and O₂^{•-} were appeared to be the dominant active species in the system. However, the addition of Bi on TiO₂ alone did not have any positive effect on the photocatalytic activity of catalyst while Pt addition, in contrast, significantly enhanced the degradation rate of MO in both Pt-TiO₂ and Bi/Pt-TiO₂ systems while decreasing the formation of •OH_{ads}. In fact, Fig. 7D shows that the introduction of Bi to Pt-TiO₂ had a synergistic effect and further enhanced the MO degradation rate compared to that of Pt-TiO₂ while decreasing the role of •OH_{bulk} and ¹O₂ in the process.

To further confirm the enhanced photocatalytic activity on these modified TiO₂, photocurrent measurements were conducted by applying +0.5 V anodic bias, as shown in Fig. 8. Pt1%-TiO₂ performed

higher photocurrent (ca. 21 μA) than pure TiO_2 (ca. 16 μA) and $\text{Bi1\%}-\text{TiO}_2$ (ca. 8 μA). Furthermore, the highest photocurrent value of ca. 35 μA was obtained on the $\text{Bi1\%}-\text{Pt1\%}-\text{TiO}_2$. These results are consistent with the results of MO degradation.

Above results indicate that the enhancement in the selective oxidation of lignin due to Bi addition may be ascribed to the higher production of $\text{O}_2^{\bullet-}$, and the lower generation of $\cdot\text{OH}$ in $\text{Bi}/\text{Pt}-\text{TiO}_2$ system. $\cdot\text{OH}$ usually acts as a non-selective radical due to its high redox potential (2.8 V, vs SHE), resulting in often complete decomposition of organic compounds. In contrast, $\text{O}_2^{\bullet-}$ is expected to result in the selective oxidation owing to its suitable redox potential (0.89 V, vs SHE) [39].

Based on the above findings, the following mechanism for the selective photo-oxidation of lignin is proposed. Since the conduction band of TiO_2 (-0.5 eV vs. NHE [40]) is more negative than the Fermi level of metal Bi (-0.17 eV, NHE), the photo-excited electrons could transfer from TiO_2 to metal Bi [41,42]. Given that the redox potential of O_2 to $\text{O}_2^{\bullet-}$ (-0.33 eV, NHE) was more positive than that of the conduction band of TiO_2 (-0.5 eV, NHE), these separated electrons would subsequently reduce O_2 to produce $\text{O}_2^{\bullet-}$ [43]. In addition, H_2O_2 was reduced by the photo-driven e^- from O_2 on the basis of the redox potential of O_2 to H_2O_2 (0.695 eV, NHE), to form $\cdot\text{OH}$ via one electron process, as shown in Eqs. (1)–(7). However, as is well known, the first step reaction is the important one to determine the reaction rate in multistep continuous reactions ($\text{O}_2 \rightarrow \text{O}_2^{\bullet-} \rightarrow \text{H}_2\text{O}_2 \rightarrow \cdot\text{OH}$) as described by Eqs. (3)–(7). Therefore, in $\text{Bi}/\text{Pt}-\text{TiO}_2$ system, more $\text{O}_2^{\bullet-}$ radicals were generated accompanying by less $\cdot\text{OH}$ production.



4. Conclusions

This work demonstrated a new Bi and Pt co-modified TiO_2 for photo-oxidation of lignin under solar light illumination to form guaiacol, vanillic acid, vanillin, 4-phenyl-1-buten-4-ol. The photocatalytic activity of $\text{Bi}/\text{Pt}-\text{TiO}_2$ was greatly enhanced compared to those of $\text{Bi}-\text{TiO}_2$ and $\text{Pt}-\text{TiO}_2$, resulting in selective oxidation of lignin. The amount of Bi and Pt had an impact on the photocatalytic selectively of $\text{Bi}/\text{Pt}-\text{TiO}_2$ with the $\text{Bi1\%}-\text{Pt1\%}-\text{TiO}_2$ exhibiting the best photocatalytic properties. The generated h^+ and $\text{O}_2^{\bullet-}$ were found to be controlling the oxidation process in $\text{Bi1\%}-\text{Pt1\%}-\text{TiO}_2$ photocatalytic system. Pt provided active sites to greatly improve the separation of photo-generated hole-electron pairs while Bi acted as a promoter to induce the generation of $\text{O}_2^{\bullet-}$ from trapped photo-electrons. This study provides new opportunities for the conversion of biomass using bismuth and noble metal-based photocatalysts under solar radiation.

In the present work, the highest observed conversion for lignin was 84.5% and the highest yield of guaiacol was 22.7% achieved over $\text{Bi1\%}-\text{Pt1\%}-\text{TiO}_2$ after 1 h irradiation. Similarly, the highest production of vanillic acid (3.5%) was observed after 1.5 h of oxidation over $\text{Bi1\%}-\text{Pt2\%}-\text{TiO}_2$. For comparison, Nakamura et al. reported complete decomposition of sodium lignosulfonate into carbon dioxide and water using ozonolysis and microbial treatment in the presence of activated sludge after 3 h [44]. Liang et al. synthesized rare earth doped TiO_2 as photocatalysts for lignin (alkali lignin) degradation

under UV light illumination [45] and reported that after 1 h of treatment, almost 70% of lignin was degraded but without formation of any valuable products. Others used pyrolysis of softwood or hardwood lignin to obtain guaiacol and syringyl derivatives [46–50]. However, photocatalytic conversion of lignin developed in this study is a useful method for producing more valuable compounds under facile environment.

Acknowledgements

This work was supported by NSERC Discovery Grant by funded by the Canada Government.

Appendix A. Supplementary data

Supplementary data associated with this article can be found, in the online version, at <http://dx.doi.org/10.1016/j.apcatb.2016.11.045>.

References

- [1] D. Ghosh, D. Dasgupta, D. Agrawal, S. Kaul, D.K. Adhikari, A.K. Kurmi, P.K. Arya, D. Bangwal, M.S. Negi, Energy Fuel 29 (2015) 3149–3157.
- [2] J.B. Binder, R.T. Raines, J. Am. Chem. Soc. 131 (2009) 1979–1985.
- [3] P. Azadi, O.R. Inderwildi, R. Farnood, D.A. King, Renew. Sust. Energy Rev. 21 (2013) 506–523.
- [4] A.K. Sinha, U.K. Sharma, N. Sharma, Int. J. Food Sci. Nutr. 59 (2008) 299–326.
- [5] G. Camera-Roda, V. Augugliaro, A. Cardillo, V. Loddo, G. Palmisano, L. Palmisano, Chem. Eng. J. 224 (2013) 136–143.
- [6] M. Ozagac, C. Bertino-Ghera, D. Uzio, M. Rivallan, D. Laurenti, C. Geantet, Biomass Bioenergy 95 (2016) 194–205.
- [7] M. Saidi, F. Samimi, D. Karimipourfard, T. Nimmanwudipong, B.C. Gates, M.R. Rahimpour, Energy Environ. Sci. 7 (2014) 103–129.
- [8] D.-Y. Hong, S.J. Miller, P.K. Agrawala, C.W. Jones, Chem. Commun. 46 (2010) 1038–1040.
- [9] C.Z. Li, X.C. Zhao, A.Q. Wang, G.W. Huber, T. Zhang, Chem. Rev. 115 (2015) 11559–11624.
- [10] S.-H. Li, S.Q. Liu, J.C. Colmenares, Y.-J. Xu, Green Chem. 18 (2016) 594–607.
- [11] J. Schneider, M. Matsuoka, M. Takeuchi, J.L. Zhang, Y. Horiuchi, M. Anpo, D.W. Bahnemann, Chem. Rev. 114 (2014) 9919–9986.
- [12] R. Rangel, G.J. Lopez Mercado, P. Bartolo-Perez, R. Garcia, Sci. Adv. Mater. 4 (2012) 573–578.
- [13] C.A.K. Gouveia, F. Wypych, S.G. Moraes, N. Duran, P. Peralta-Zamora, Chemosphere 40 (2000) 427–432.
- [14] Y.-S. Ma, C.-N. Chang, Y.-P. Chiang, H.-F. Sung, A.C. Chao, Chemosphere 71 (2008) 998–1004.
- [15] Y. Shiraihi, H. Sakamoto, K. Fujiwara, S. Ichikawa, T. Hirai, ACS Catal. 4 (2014) 2418–2425.
- [16] H. Li, Z. Lei, C. Liu, Z. Zhang, B. Lu, Bioresour. Technol. 175 (2015) 494–501.
- [17] J.G. Wang, P.H. Rao, W. An, J.L. Xu, Y. Men, Appl. Catal. B 195 (2016) 141–148.
- [18] X.Y. Pan, Y.-J. Xu, J. Phys. Chem. C 117 (2013) 17996–18005.
- [19] A. Zalineeva, A. Serov, M. Padilla, U. Martinez, K. Artyushkova, S. Baranton, C. Coutanceau, P.B. Atanassov, J. Am. Chem. Soc. 136 (2014) 3937–3945.
- [20] M.C. Figueiredo, R.M. Arán-Ais, J.M. Feliu, K. Kontturi, T. Kallio, J. Catal. 312 (2014) 78–86.
- [21] T. Lu, Z. Du, J. Liu, H. Ma, J. Xu, Green Chem. 15 (2013) 2215–2221.
- [22] C. Mondelli, D. Ferri, J. Grunwaldt, F. Krumeich, S. Mangold, R. Psaro, A. Baiker, J. Catal. 252 (2007) 77–87.
- [23] R. Nie, D. Liang, L. Shen, J. Gao, P. Chen, Z. Hou, Appl. Catal. B 127 (2012) 212–220.
- [24] T. Mallat, Z. Bodnar, A. Baiker, O. Greis, H. Strubig, A. Reller, J. Catal. 142 (1993) 237–253.
- [25] Y. Kwon, Y. Birdja, I. Spanos, P. Rodriguez, M.T.M. Koper, ACS Catal. 2 (2012) 759–764.
- [26] X.M. Ning, Y.H. Li, H. Yu, F. Peng, H.J. Wang, Y.H. Yang, J. Catal. 335 (2016) 95–104.
- [27] H.F. Li, Z.F. Lei, C.G. Liu, Z.Y. Zhang, B.W. Lu, Bioresour. Technol. 175 (2015) 494–501.
- [28] K. Tanaka, R.C.R. Calanag, T. Hisanaga, J. Mol. Catal. A Chem. 138 (1999) 287–294.
- [29] L.Q. Jing, B.F. Xin, F.L. Yuan, L.P. Xue, B.Q. Wang, H.G. Fu, J. Phys. Chem. B 110 (2006) 17860–17865.
- [30] W.P. Deng, H.X. Zhang, X.J. Wu, R.S. Li, Q.H. Zhang, Y. Wang, Green Chem. 17 (2015) 5009–5018.
- [31] P. Ding, M. Garrett, Ø. Loe, A.W. Nienow, A.W. Pacek, Ind. Eng. Chem. Res. 51 (2012) 184–188.
- [32] N. Xu, T. Takei, A. Miura, N. Kumada, K.-I. Katsumata, N. Matsushita, K. Okada, Langmuir 31 (2015) 7660–7665.
- [33] T.T. Zhang, S.T. Wang, F. Chen, J. Phys. Chem. C 120 (2016) 9732–9739.

- [34] T. Mallat, Z. Bodnar, P. Hug, A. Baiker, *J. Catal.* 153 (1995) 131–143.
- [35] Z. Sun, J. Guo, S. Zhu, L. Mao, J. Ma, D. Zhang, *Nanoscale* 6 (2014) 2186–2193.
- [36] J. Ren, W.Z. Wang, S.M. Sun, L. Zhang, J. Chang, *Appl. Catal. B* 92 (2009) 50–55.
- [37] Y.B. Ding, F. Yang, L.H. Zhu, N. Wang, H.Q. Tang, *Appl. Catal. B* 164 (2015) 151–158.
- [38] J. Wang, P. Wang, Y. Cao, J. Chen, W. Li, Y. Shao, Y. Zheng, D. Li, *Appl. Catal. B* 136–137 (2013) 94–102.
- [39] W. Feng, G.J. Wu, L.D. Li, N.J. Guan, *Green Chem.* 13 (2011) 3265–3272.
- [40] Z.H.N. Al-Azri, W.-T. Chen, A. Chan, V. Jovic, T. Ina, H. Idriss, G.I.N. Waterhouse, *J. Catal.* 329 (2015) 355–367.
- [41] F. Dong, Q. Li, Y. Sun, W.-K. Ho, *ACS Catal.* 4 (2014) 4341–4350.
- [42] A. Furube, L. Du, K. Hara, R. Katoh, M. Tachiya, *J. Am. Chem. Soc.* 129 (2007) 14852–14853.
- [43] F. Dong, Q.Y. Li, Y.J. Sun, W.K. Ho, *ACS Catal.* 4 (2014) 4341–4350.
- [44] Y. Nakamura, M. Daidai, F. Kobayashi, *Water Sci. Technol.* 50 (2004) 167–172.
- [45] L. Song, X.Y. Zhao, L.X. Cao, J.-W. Moon, B.H. Gu, W. Wang, *Nanoscale* 7 (2015) 16695–16703.
- [46] D.Y. Hong, S.J. Miller, P.K. Agrawal, C.W. Jones, *Chem. Commun.* 46 (2010) 1038–1040.
- [47] C. Zhao, Y. Kou, A.A. Lemonidou, X.B. Li, J.A. Lercher, *Angew. Chem. Int. Ed.* 48 (2009) 3987–3990.
- [48] T. Nimmanwudipong, R.C. Runnebaum, D.E. Block, B.C. Gates, *Catal. Lett.* 141 (2011) 779–783.
- [49] X. Zhu, R.G. Mallison, D.E. Resasco, *Appl. Catal. A* 379 (2010) 172–181.
- [50] M.A. Gonzalez-Borja, D.E. Resasco, *Energy Fuels* 25 (2011) 4155–4162.